Inorg. Chem. **2004**, *43*, 4595–4603

Syntheses of the 47 Electron Clusters $[(Cp^*Fe)_3(\mu_3\text{-}X)_2]$ (X = S, Se) and the First Fe/Sn/Se Heterocubane Cluster $[(Cp^*Fe)_3(SnCl_3)(\mu_3\text{-}Se)_4]\cdot DME$ by the Use of Chalcogenostannate Salts

Christian Zimmermann,[†] Christopher E. Anson,[†] Amanda L. Eckermann,[‡] Markus Wunder,[‡] Gerda Fischer,[§] Ilka Keilhauer,[§] Erik Herrling,[§] Bernd Pilawa,[§] Oliver Hampe,[||] Florian Weigend,[||] and Stefanie Dehnen*[,†]

Institut für Anorganische Chemie, Universität Karlsruhe (TH), D-76128 Karlsruhe, Germany, Department of Chemistry, Northwestern University, Evanston, Illinois 60208, Physikalisches Institut, Universität Karlsruhe (TH), D-76128 Karlsruhe, Germany, and Institut für Nanotechnologie, Forschungszentrum Karlsruhe GmbH, D-76021 Karlsruhe, Germany

Received July 25, 2003

By reacting 1-aminoethylammonium ($H_2NCH_2CH_2NH_3^+$ = *en*H$^+$) salts of $[Sn_2E_6]^{4-}$ anions (E = S, Se), $[enH]_4[Sn_2S_6]$ (**1**) and $[enH]_4[Sn_2Se_6]\cdot en$ (**2**), with $FeCl_2$/LiCp*, three novel (partly) oxidized, Cp* ligated iron chalcogenide clusters were synthesized. Two of them, $[(Cp^*Fe)_3(\mu_3\text{-}S)_2]$ (**3**) and $[(Cp^*Fe)_3(\mu_3\text{-}Se)_2]$ (**4**), contain formally 47 valence electrons. $[(Cp^*Fe)_3(SnCl_3)(\mu_3\text{-}Se)_4]\cdot DME$ (**5**) represents the first known mixed metal Fe/Sn/Se heterocubane type cluster. Compounds **3**–**5** were structurally characterized by single-crystal X-ray diffraction, and the odd valence electron number of the $[Fe_3E_2]$ clusters (E = S, Se) was confirmed by density functional (DFT) investigations, mass spectrometry, cyclic voltammetry and a susceptibility measurement of **3**.

Introduction

A large number of chalcogenido bridged polynuclear iron complexes have been synthesized and characterized during the past decades.[1] The most frequently observed structural motif is the heterocubane unit.[2] Adamantane type aggregates,[3] hexagonal prisms,[4] and square pyramids[5] represent other common Fe−E subunits (E = S, Se, Te). The complexes, most of which are sulfur bridged, are usually terminally ligated in order to inhibit formation of extended solids and to provide suitable electron numbers at the iron centers; typical ligands are CO, NO, CN, or NCR groups, amines or phosphines, halides, cyclopentadienyl groups (Cp^R), or chalcogenolato ligands RE^- (R = organic group, H; E = S, Te).

In contrast, trigonal bipyramidal structures of the general type $[L_nFe_3(\mu_3\text{-}E)_2]^{q(+/-)}$ (L: terminal ligand), frequently observed with transition metal elements of a higher electron number, are rare in the coordination chemistry of iron due to the low number of cluster electrons that result from only

* Author to whom correspondence should be addressed. Tel.: Int + 721/608-2850. Fax: Int + 721/608-7021. E-mail: dehnen@chemie.uni-karlsruhe.de.

[†] Institut für Anorganische Chemie, Universität Karlsruhe (TH).

[‡] Northwestern University.

[§] Physikalisches Institut, Universität Karlsruhe (TH).

[||] Forschungszentrum Karlsruhe GmbH.

(1) Reviews: (a) Ogino, H.; Inomata, S.; Tobita, H. *Chem. Rev.* **1998**, *98*, 2093-2121. (b) Dance, I. G.; Fisher, K. *Prog. Inorg. Chem.* **1994**, *41*, 637−803. (c) Harris, S. *Polyhedron* **1989**, *8*, 2843−2882. (d) Berg, J. M.; Holm, R. H. In Spiro, T. G. (Ed.), *Iron−Sulfur Proteins*; Spiro, T. G., Ed.; John Wiley and Sons: New York, 1982; p 1.

(2) Recent publications on $[Fe_4E_4]$ clusters: (a) Zhou, H. C.; Holm, R. H. *Inorg. Chem.* **2003**, *42*, 11−21. (b) Zhu, N.; Appelt, R. Vahrenkamp, H. *J. Organomet. Chem.* **1998**, *565*, 187−192. (c) Davies, S. C.; Evans, D. J.; Henderson, R. A.; Hughes, D. L.; Longhurst, S. *J. Chem. Soc., Dalton Trans.* **2001**, 3470−3477. (d) Segal, B. M.; Hoveyda, H. R.; Holm, R. H. *Inorg. Chem.* **1998**, *37*, 3440−3443. (e) Han, J.; Coucouvanis, D. *Inorg. Chem.* **2002**, *41*, 2738−2746. (f) Hauptmann, R.; Schneider, J.; Chen, C.; Henkel, G. *Acta Crystallogr.* **1999**, *C55*, 192−194. (g) Steigerwald, M. L.; Siegrist, T.; Gyorgy, E. M.; Hessen, B.; Kwon, Y.-U.; Tanzler, S. M. *Inorg. Chem.* **1994**, *33*, 3389−3395.

(3) Recent publication on $[Fe_4S_6]$ clusters: Harmjanz, M.; Junghans, C.; Opitz, U.-A.; Bahlmann, B.; Pohl, S. *Z. Naturforsch.* **1996**, *B51*, 1040−1048.

(4) Recent publications on $[Fe_6E_6]$ clusters: (a) Goddard, C. A.; Ling, J. R.; Holm, R. H. *Inorg. Chem.* **1996**, *35*, 4347−4354. (b) Cecconi, F.; Gilhardi, C. A.; Midollini, S.; Orlandini, A. *Inorg. Chim. Acta* **1997**, *254*, 387−389.

(5) Recent publications on square pyramidal $[Fe_3E_2]$ clusters: (a) Zheng, H.-B.; Miao, S.-B.; Wang, Z.-X.; Zhou, Z.-Y.; Zhou, X.-G. *Polyhedron* **2000**, *19*, 713−718. (b) Cauzzi, D.; Graiff, C.; Lanfranchi, A.; Predieri, G.; Tripicchio, A. *J. Organomet. Chem.* **1997**, *536*, 497−507. (c) Seidel, R.; Schnautz, B.; Henkel, G. *Angew. Chem., Int. Ed. Engl.* **1996**, *35*, 1710−1712. (d) Rheingold, A. L.; Ostrander, R. L.; Mathur, P. *Acta Crystallogr.* **1993**, *C49*, 1741−1743.

10.1021/ic034876t CCC: $27.50 © 2004 American Chemical Society
Published on Web 06/26/2004

Scheme 1. Syntheses of Iron Chalcogenide Clusters **3**−**5**

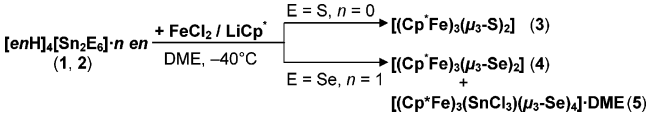

two bridging ligands per three iron atoms. The only examples so far isolated are the clusters $[\{(CO)_3Fe\}_3(\mu_3\text{-}CO)(\mu_3\text{-}S)]$ (48 valence electrons),[6] $[(Cp^*Fe)_2(CO)_3Fe(\mu_3\text{-}S)_2]$ (48 valence electrons),[7] $[(Cp^*Fe)_2\{(CO)_2(PPh_3)Fe\}(\mu_3\text{-}S)_2]^+$ (47 valence electrons),[8] and the edge-sharing trigonal bipyramids in $[(\{CO\}_3Fe)_2(\mu_3\text{-}S)_2Fe(\mu_3\text{-}S)_2(CpCr)_2(\mu_2\text{-}StBu)]$.[9] Analogous selenium or tellurium bridged pentanuclear iron clusters are only known in the more common square pyramidal shape at 50 valence electrons.

In the course of our studies of the reactivity of chalcogenostannate anions toward pentamethylcyclopentadienyl (Cp*) coordinated transition metal complexes, we recently reported the mild oxidation potential of chalcogenostannate compounds $K_6Sn^{III}_2Se_6$[10a] and $Li_4Sn^{IV}_2Te_6{\cdot}8en$,[10b] that allowed for the novel synthesis of Cp* ligated mixed valence cobalt selenide clusters[11a] and the first Cp* coordinated cobalt telluride cluster.[11b] However, the use of these chalcogeno stannate salts proved to be unsuitable for the synthesis and isolation of crystalline iron complexes or sulfur bridged compounds in general. Therefore, it was decided to replace the alkali metal counterions by $[RNH_3]^+$ ions. Such salts ought to react less rapidly toward transition metal complex halides, both because the formation of alkaline metal halide ceases to be the driving force and because the crystal packing is characterized by numerous hydrogen bonds that lead to an additional stabilization of the reactant. Protonated *en* molecules (*en* = 1,2-diaminoethane) were found to be appropriate counterions that are readily incorporated in the crystal lattices.[12]

Results and Discussion

Syntheses. By reacting recently reported 1-aminoethylammonium salts of $[Sn_2E_6]^{4-}$ anions, $[enH]_4[Sn_2S_6]$ (**1**) and $[enH]_4[Sn_2Se_6]{\cdot}en$ (**2**),[12] with $FeCl_2$/LiCp*, we obtained two novel Cp* ligated, mixed valence 47 electron clusters with trigonal bipyramidal cores, $[(Cp^*Fe)_3(\mu_3\text{-}S)_2]$ (**3**) and $[(Cp^*Fe)_3(\mu_3\text{-}Se)_2]$ (**4**), and a mixed metal Fe/Sn/Se heterocubane type cluster, $[(Cp^*Fe)_3(SnCl_3)(\mu_3\text{-}Se)_4]{\cdot}$DME (**5**), as shown in Scheme 1.

Table 1. Crystallographic Data for Compounds **3**, **4**, and **5**

	3	**4**	**5**
empirical formula	$C_{30}H_{45}Fe_3S_2$	$C_{30}H_{45}Fe_3Se_2$	$C_{34}H_{55}Cl_3Fe_3O_2Se_4Sn$
ffw/g·mol^{-1}	637.33	731.13	1204.21
cryst description	black block	dark purple chunk	black block
cryst size /mm^3	0.25 × 0.15 × 0.10	0.08 × 0.05 × 0.04	0.04 × 0.02 × 0.02
cryst syst	monoclinic	monoclinic	orthorhombic
space group	$P2_1/n$	$P2_1/n$	*Pnma*
a/Å	10.7498(6)	10.8202(5)	21.3716(10)
b/Å	17.9645(9)	18.0569(9)	16.5989(8)
c/Å	16.1820(8)	16.1900(8)	22.8810(11)
β/deg	107.975(1)	107.524(1)	
V/Å^3	2972.5(3)	3016.4(3)	8116.9(7)
Z	4	4	8
ρ_{calc}/g·cm^{-3}	1.424	1.610	1.971
μ(Mo Kα)/mm^{-1}	1.602	3.854	5.474
2Θ range/deg	3−56	3−56	3−57
reflns collected	18588	15117	49053
indep reflns	6717	6797	9697
R(int)	0.0343	0.0290	0.2070
indep reflns with $I > 2\sigma(I)$	5311	5340	3720
parameters	332	332	465
largest diff peak/hole/ e$^-$·Å^{-3}	0.585/−0.571	0.544/−0.588	2.373/−1.867
T_{min}/T_{max}	0.516/0.801	0.621/0.801	0.45/1.00
GOF (F^2)	0.975	1.013	0.861
R_1	0.0366	0.0309	0.0717
wR_2	0.0856	0.0782	0.1699

Compounds **3**−**5** are gained in relatively low yields (26%, 16%, 1%, respectively). However, until now the described method seems to be the only route yielding these compounds; attempts to vary and improve the synthesis by alternative synthetic pathways were not successful yet. For instance, reactions of $FeCl_2$/LiCp* with NaEH or Na_2E (E = S, Se) resulted in the very rapid formation of the binary chalcogenides. Obviously both the oxidative effect of the stannate compounds and the slow liberation of E^{2-} from the used $[enH]^+$ salts was necessary for isolation of the Cp* ligated clusters described here.

Compounds **3**−**5** were structurally characterized by single-crystal X-ray diffraction; the composition of the trigonal bipyramidal clusters **3** and **4** and, thus, the odd electron number (47) were confirmed by density functional theoretical (DFT) investigations,[13] by mass spectrometry, by electrochemical investigations, and by measurement of the magnetic susceptibility of **3**.[14]

Crystal Structures. Table 1 lists the data of the X-ray diffractometry measurements of $[(Cp^*Fe)_3(\mu_3\text{-}S)_2]$ (**3**), $[(Cp^*Fe)_3(\mu_3\text{-}Se)_2]$ (**4**), and $[(Cp^*Fe)_3(SnCl_3)(\mu_3\text{-}Se)_4]{\cdot}$DME (**5**).

Crystal Structures of $[(Cp^*Fe)_3(\mu_3\text{-}S)_2]$ (3) and $[(Cp^*Fe)_3(\mu_3\text{-}Se)_2]$ (4). Compounds **3** and **4** crystallize isotypically in

(6) Markó, L.; Madach, T.; Vahrenkamp, H. *J. Organomet. Chem.* **1980**, *190*, C67−C70.
(7) Mitsui, T.; Inomata, S.; Ogino, H. *Inorg. Chem.* **1994**, *33*, 4934−4936.
(8) Yuki, M.; Mitsui, T.; Inomata, S.; Okazaki, M.; Ogino, H. *Chem. Lett.* **1998**, 561−562.
(9) Eremenko, I. L.; Pasinskii, A. A.; Katugin, A. S.; Zalmanovitch, V. R.; Orazsakhatov, B.; Sleptsova, S. A.; Nekhaev, A. I.; Kaverin, V. V.; Ellert, O. G.; Novotortsev, V. M.; Yanovsky, A. I.; Shklover, V. E.; Struchkov, Y. T. *J. Organomet. Chem.* **1989**, *365*, 325−340.
(10) (a) Zimmermann, C.; Dehnen, S. *Z. Anorg. Allg. Chem.* **1999**, *625*, 1963−1965. (b) Dehnen, S.; Zimmermann, C.; Anson, C. E. *Z. Anorg. Allg. Chem.* **2002**, *628*, 279−288.
(11) (a) Dehnen, S.; Zimmermann, C. *Chem. Eur. J.* **2000**, *6*, 2256−2261. (b) Zimmermann, C.; Dehnen, S. *Z. Allg. Anorg. Chem.* **2001**, *627*, 847−850.
(12) Zimmermann, C.; Dehnen, S. *Z. Allg. Anorg. Chem.* **2002**, *628*, 2463−2469.
(13) (a) Parr, R. G.; Yang, W. *Density Functional Theory of Atoms and Molecules*; Oxford University Press: New York 1988. (b) Ziegler, T. *Chem. Rev.* **1991**, *91*, 651−667.
(14) Compound **5** crystallizes in very small amounts besides **4**. The crystals precipitate always in a drop of a simultaneously formed, oily liquid which remains on the surface on the crystals upon isolation and leads to rapid deliquescence. Once isolated, the material is soluble in all common organic solvents; thus it is neither possible to wash the crystals nor to recrystallize **5**. Therefore, further solid state characterization of **5** beyond its crystal structure, such as Mössbauer spectroscopy, was not possible to date.

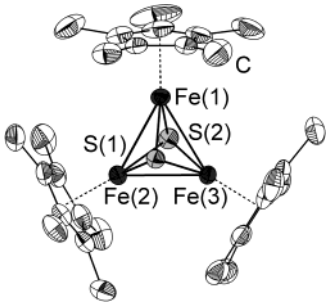

Figure 1. Thermal ellipsoid diagram of the molecular structure of $[(Cp^*Fe)_3(\mu_3\text{-}S)_2]$ (**3**); H atoms omitted for clarity. Ellipsoids are drawn to 50% probability.

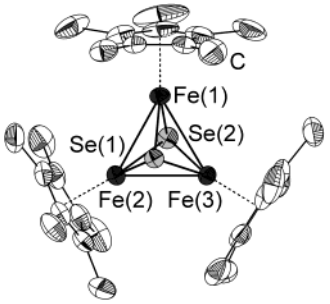

Figure 2. Thermal ellipsoid diagram of the molecular structure of $[(Cp^*Fe)_3(\mu_3\text{-}Se)_2]$ (**4**); H atoms omitted for clarity. Ellipsoids are drawn to 50% probability.

Table 2. Selected Distances [Å] and Angles [deg] for **3** (E = S) and **4** (E = Se)

	3 (E = S)	**4** (E = Se)
Fe−E	2.1664(6)−2.1741(6)	2.2866(4)−2.2987(4)
Fe−C	2.088(3)−2.137(2)	2.092(2)−2.139(2)
Fe(1)−Fe(2)	2.6233(4)	2.6979(5)
Fe(1)−Fe(3)	2.6183(5)	2.6982(5)
Fe(2)−Fe(3)	2.5965(4)	2.6575(5)
$Fe-Fe_{av}$	2.6127	2.6845
E−Fe(1)−E	92.12(2)	95.206(16)
E−Fe(2,3)−E	91.86(2), 91.98(2)	94.671(15), 94.906(15)
Fe(1)−E−Fe	74.14(2)−74.39(2)	72.080(14)−72.218(14)
Fe(2)−S−Fe(3)	73.37(2), 73.42(2)	70.735(14), 70.749(14)

the monoclinic space group $P2_1/n$ with four formula units in the unit cell. Figures 1 and 2 show the molecular structures of **3** and **4** in the crystal; respective structural parameters are summarized in Table 2.

The molecular structures of both **3** and **4** are based on a distorted trigonal $[Fe_3E_2]$ bipyramid (E = S, Se; C_1 site symmetry). This structural motif is typical for 48 valence electron pentanuclear clusters as predicted by Wade−Mingos rules.[15] Accordingly, it is observed for all known 48 electron clusters, among them the only two structurally characterized iron species mentioned earlier, $[\{(CO)_3Fe\}_3(\mu_3\text{-}CO)(\mu_3\text{-}S)]$[6] or $[(Cp^*Fe)_2(CO)_3Fe(\mu_3\text{-}S)_2]$.[7] However, the neutral complexes **3** and **4** formally contain two Fe^{II} centers and one Fe^{III} ion, resulting in a 47 valence electron count. The formal loss of one electron from the HOMO of an ideal trigonal bipyramidal 48 electron cluster should lead to a distortion, i.e. elongation of one Fe−Fe contact if the lost electron is removed from an Fe−Fe bonding orbital, or shortening and

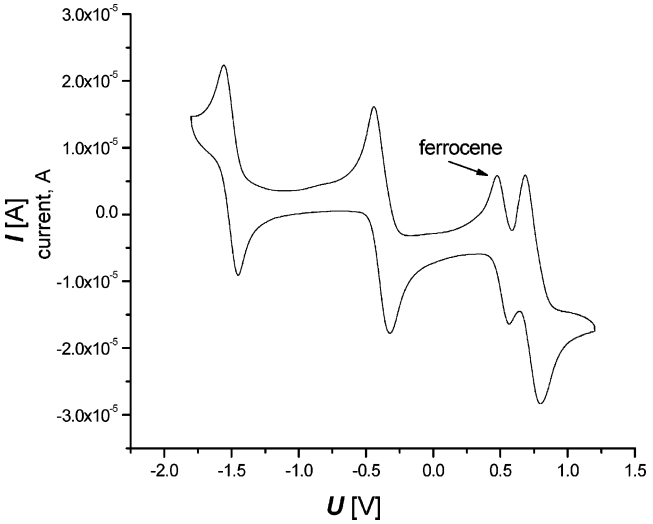

Figure 3. Cyclic voltammogram of **3** (c = 1.5 mmol·L^{-1} in CH_2Cl_2) and ferrocene. The scan rate is 0.100 V·s^{-1}, and the reference electrode is Ag/AgCl.

corresponding increase of the Fe−Fe bond order if an Fe−Fe antibonding orbital is concerned. Indeed, one observes one shorter Fe−Fe contact (Fe(2)−Fe(3): 2.5965(4) Å in **3**; 2.6575(5) Å in **4**) besides two longer ones (2.6233(4), 2.6183(5) Å in **3**; 2.6979(5), 2.6982(5) Å in **4**), indicating removal of the electron from an Fe_3 antibonding HOMO, but the distortion is not very distinct.

Only one 47 electron cluster has been crystallographically characterized to date, $[(Cp^*Fe)_2\{(CO)_2(PPh_3)Fe\}(\mu_3\text{-}S)_2]^+$,[8] which shows a somewhat larger Fe−Fe bond range (2.596(1), 2.622(1), 2.663(1) Å); as in **3** or **4**, the three Fe−Fe contacts do not follow the expected distortion pattern. However, the average Fe−Fe distance (2.627) is very similar to that in **3**. Comparison of the structural data of **3** with the quoted 48 electron iron sulfide cluster $[Cp^*_2(CO)_3Fe_3(\mu_3\text{-}S)_2]$ (Fe−Fe, 2.601(1)−2.704(1) Å; Fe−S, 2.139(2)−2.290(1) Å)[6] again demonstrates the lower electron number in **3**.

The only structurally determined iron selenide compounds with five cluster atoms are $[\{(CO)_3Fe\}_3(\mu_3\text{-}Se)_2]$[16] and $[\{(CO)_3Fe\}_3(\mu_3\text{-}E)(\mu_3\text{-}Se)]$ (E = S, Te)[17] that contain 50 valence electrons and accordingly adopt a square pyramidal Fe_3E_2 core such as sulfide analogue $[\{(CO)_3Fe\}_3(\mu_3\text{-}S)_2]$.[18] Due to the lack of structurally related 47 or 48 electron species, it is not possible to comment on the structural parameters in **4**. However, since it is isotypic to **3** and shows an even larger bond length discrepancy, the formulation of **4** as a 47 electron cluster also seems to be correct.

Electrochemical Investigations of $[(Cp^*Fe)_3(\mu_3\text{-}S)_2]$ (3). We investigated the electrochemical behavior of compound **3** that crystallizes selectively and can therefore be isolated as pure material. The cyclic voltammogram of **3** (Figure 3) shows three one-electron redox events corresponding to one reduction and two oxidations at −2.010, −0.910, and +0.197

(15) (a) Wade, K. *Adv. Inorg. Chem.* **1976**, *18*, 1−66. (b) Mingos, D. M. P. *Acc. Chem. Res.* **1984**, *17*, 311−319. (c) Mingos, D. M. P.; Johnston, R. L. *Struct. Bonding* **1987**, *68*, 29−87.

(16) Dahl, L. F.; Sutton, P. W. *Inorg. Chem.* **1963**, *2*, 1067−1069.
(17) Gervasio, G. *J. Organomet. Chem.* **1993**, *445*, 147−155.
(18) (a) Madach, T.; Vahrenkamp, H. *Chem. Ber.* **1981**, *114*, 505−512. (b) Pullian, C. R.; Thoden, J. B.; Stacy, M. S.; Spencer, B.; Englert, M. H., Dahl, L. F. *J. Am. Chem. Soc.* **1991**, *113*, 7398−7410.

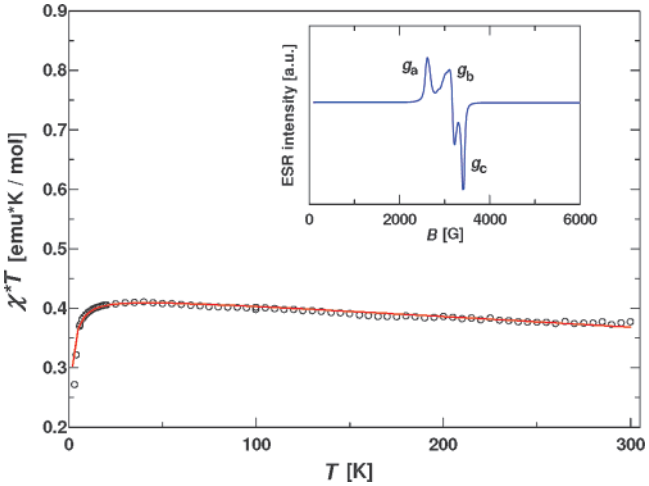

Figure 4. χT versus T plot observed by a static magnetic susceptibility measurement of **3** at a field strength of 10 kOe. The inset shows an ESR signal of **3** at $\nu = 9.5$ GHz and $T = 5$ K.

V relative to an internal $Fc^{+/0}$ standard. The events are reversible on the basis of peak separation ($E_{pa} - E_{pc}$) and the i_a/i_c ratios vs the internal $Fc^{+/0}$ standard (+0.519 vs Ag/AgCl). The data show that the $Fe(III)_3$, $Fe(III)_2Fe(II)$, and $Fe(II)_3$ states are accessible. The reduced species $[(Cp^*Fe)_3(\mu_3\text{-}S)_2]^-$, in which all the iron centers are formally Fe(II), has 48 electrons. This species may be chemically generated and isolated for further characterization. As electrochemical data were not included with previous reports of 47 and 48 electron Fe−S clusters, no comparisons may be drawn. However, the observed potentials are similar to the Fe(III)/Fe(II) transition reported for $[Cp_4Fe_4S_4]^{2+}$.[26b] Comparison to the electrochemistry of related clusters $[(CpCo)_3(\mu_3\text{-}S)_2]$ (0/−, −1.13 V; 0/+, −0.12 V; +/2+, +0.57 V),[18a] $[(Cp'Co)_3(\mu_3\text{-}S)_2]$ (0/−, −1.31 V; 0/+, −0.26 V; +/2+, +0.52 V),[18b] or $[(Cp^*Co)_3(\mu_3\text{-}Se)_2]$ (0/+, −0.54 V; +/2+, +0.13 V)[11a] reflects the shift toward facilitation of the oxidation in **3** as expected for the less noble Fe compound.

Static Magnetic Susceptibility of $[(Cp^*Fe)_3(\mu_3\text{-}S)_2]$ (3). In order to experimentally check the odd electron number and to determine the ground state of the 47 electron compounds, the static magnetic susceptibility of the Fe−S species **3** was measured with a SQUID magnetometer. Figure 4 shows the graph of χT versus T and an ESR signal at $\nu = 9.5$ GHz and $T = 5$ K.

(19) Kabashima, S.-i.; Kuwata, S.; Ueno, K.; Shiro, M.; Hidai, M. *Angew. Chem., Int. Ed.* **2000**, *20*, 1128−1131.
(20) Zhang, Y.-P.; Baskin, J. K.; Holm, R. H. *Inorg. Chem.* **1987**, *26*, 694−702.
(21) Chu, C. T.-W.; Lo, F. Y.-K.; Dahl, L. F. *J. Am. Chem. Soc.* **1982**, *104*, 3409−3422.
(22) Fedin, V. P.; Sokolv, M. N.; Virovets, A. V.; Podberezskaya, N. V.; Fedorov, V. E. *Inorg. Chim. Acta* **1998**, *269*, 292−296.
(23) Saysell, D. M.; Lamprecht, G. J.; Darkwa, G. J.; Sykes, A. G. *Inorg. Chem.* **1996**, *35*, 5531−5535.
(24) Hernandez-Molina, R.; Dybtsev, D. N.; Fedin, V. P.; Elsegood, M. R. J.; Clegg, W.; Sykes, A. G. *Inorg. Chem.* **1998**, *37*, 2995−3001.
(25) (a) Varey, J. E.; Lamprecht, G. J.; Fedin, V. P.; Holder, A.; Clegg, W.; Elsegood, M. R. J.; Sykes, A. G. *Inorg. Chem.* **1996**, *35*, 5525−5530; (b) Keck, H.; Kruse, A.; Kuchen, W.; Mootz, D.; Wiskemann, R.; Wunderlich, H. *Z. Naturforsch.* **1990**, *45b*, 461−464.
(26) (a) Trinh-Toan; Fehlhammer, P. W.; Dahl, L. F. *J. Am. Chem. Soc.* **1977**, *99*, 402−407. (b) Trinh-Toan; Teo, B. K.; Ferguson, J. A.; Meyer, T. J.; Dahl, L. F. *J. Am. Chem. Soc.* **1977**, *99*, 408−416.

Table 3. Calculated Fe−Fe Distances [Å] of 47 Electron Clusters $\mathbf{3}_{calc}$ and $\mathbf{4}_{calc}$ and the Hypothetical 48 Electron Analogues $[\mathbf{3}_{calc}]^-$ and $[\mathbf{4}_{calc}]^-$

	$\mathbf{3}_{calc}$	$\mathbf{4}_{calc}$	$[\mathbf{3}_{calc}]^-$	$[\mathbf{4}_{calc}]^-$
E	S	Se	S	Se
no. of valence e^-	47	47	48	48
Fe(1)−Fe(2)	2.510	2.568	2.691	2.791
Fe(1)−Fe(3)	2.708	2.805	2.692	2.792
Fe(2)−Fe(3)	2.717	2.808	2.692	2.792
$(Fe-Fe)_{av}$	2.643	2.727	2.691	2.792

The magnetic susceptibility follows a Curie−Weiss law $\chi(T) = C/(T - \Theta) + \chi_{offset}$, with the Curie constant $C = (0.425 \pm 0.004)$ emu·K/mol and the Curie−Weiss temperature $\Theta = (-0.8 \pm 0.2)$ K which indicates a small antiferromagnetic intercluster coupling. Electron spin resonance measurements at $\nu = 9.5$ GHz and $T = 5$ K of a polycrystalline sample reveal the **g**-tensor components $g_a = 2.009 \pm 0.018$, $g_b = 2.133 \pm 0.020$, and $g_c = 2.426 \pm 0.044$. With a mean g value of 2.189 ± 0.027 of the $S = {}^1/_2$ ground state of cluster **3** the expected value of C is 0.449 emu·K/mol. Thus the obtained value of the Curie constant is in good agreement with this and indicates that about 95% of **3** carry a magnetic moment. The small rest of the probe is obviously diamagnetic. χ_{offset} includes the temperature independent core susceptibility $\chi_c = (-4.2 \pm 0.1) \times 10^{-4}$ emu/mol and the contribution of a magnetic impurity $M_{impurity} = (3.72 \pm 0.07) \times 10^{-3}$ G·emu/g which is caused by small but not negligible ferromagnetic or ferrimagnetic contamination of the sample (e.g. 52 μg of Fe_2O_3, which corresponds to 1% of the total mass of the sample).

DFT Investigations of $[(Cp^*Fe)_3(\mu_3\text{-}S)_2]$ (3) and $[(Cp^*Fe)_3(\mu_3\text{-}Se)_2]$ (4). By computational treatment of the 47 electron clusters using density functional (DFT) methods,[13] we calculated a doublet ground state ($S = {}^1/_2$) for both $\mathbf{3}_{calc}$ and $\mathbf{4}_{calc}$ in accordance with the magnetic susceptibility measurements.

In order to rationalize the shortening of one Fe−Fe contact, i.e. to check whether the HOMO of a related 48 electron species would be antibonding with respect to the $[Fe_3]$ ring, we additionally calculated the 48 electron analogues $[\mathbf{3}_{calc}]^-$ and $[\mathbf{4}_{calc}]^-$. Fe−Fe distances of the calculated molecules are given in Table 3.

The calculations show that the removal of one electron from the hypothetical 48 electron analogues indeed affects only one Fe−Fe bond each and does not equally affect all Fe−Fe distances. However, in disagreement with the experimentally found structures, the calculated splitting of Fe−Fe bond lengths amounts to at least 0.2 Å in the optimized structures of $\mathbf{3}_{calc}$ and $\mathbf{4}_{calc}$. It is difficult to decide whether this is the result of a systematical error in the DFT structures—a larger splitting of calculated metal−metal bond distances with respect to experimentally observed ones has also been observed in DFT investigations of related Co−Se clusters[11a]—or whether the $[Fe_3]$ rings in the experimental structures are less significantly distorted due to packing effects that mainly affect the relatively weak Fe−Fe bonds (an equalization due to dynamical disorder is not reflected in the crystal structures). However, the calculated mean distances, $(Fe-Fe)_{av}$, are only slightly longer by a typical

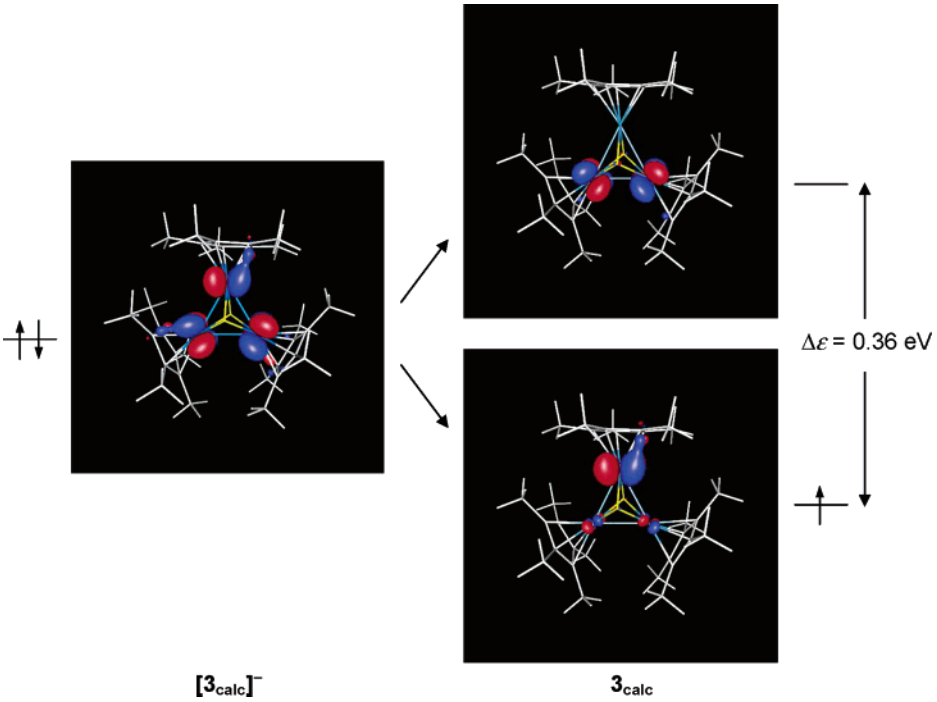

Figure 5. Representation of the doubly occupied HOMO of the calculated closed-shell species $[\mathbf{3}_{calc}]^-$ (*pseudo* C_{3h} symmetry; left-hand side) and related unrestricted-Hartree−Fock (UHF) orbitals of the open shell species $\mathbf{3}_{calc}$ (*pseudo* C_{2v} symmetry; right-hand side); orbitals are drawn to 0.38 $e^-\cdot Å^{-3}$.

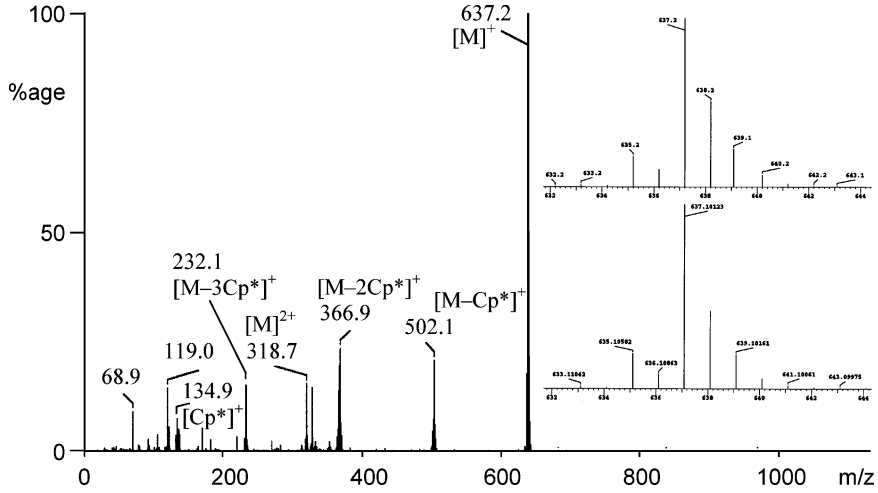

Figure 6. Mass spectrum of **3** (70 eV, 140 °C). The inset shows the isotopic distribution of the observed molecular peak (top) in comparison to the simulated pattern (bottom).

value of 0.03−0.04 Å compared to those of the clusters **3**, **4**, and also $[(Cp^*Fe)_2\{(CO)_2(PPh_3)Fe\}(\mu_3\text{-}S)_2]^+$.[8] This deviation is about the same as found for the Fe−E and Fe−C distances in the calculated clusters $\mathbf{3}_{calc}$ and $\mathbf{4}_{calc}$ with respect to the experimentally observed ones (Δ_{max}Fe−E and Δ_{max}Fe−C: 0.01 Å for $\mathbf{3}_{calc}$ vs **3**, 0.02 Å for $\mathbf{4}_{calc}$ vs **4**).

Comparison of the structural parameters of $\mathbf{3}_{calc}$ or $\mathbf{4}_{calc}$ to those in $[\mathbf{3}_{calc}]^-$ or $[\mathbf{4}_{calc}]^-$ indeed shows a shortening of one Fe−Fe contact besides two nearly unchanged Fe−Fe bonds upon removal of one electron. For the Fe−S species as an example, Figure 5 (left-hand side) displays the doubly occupied closed-shell HOMO of the 48 electron cluster $[\mathbf{3}_{calc}]^-$ which is antibonding with respect to the $[Fe_3]$-ring. Upon removal of one electron, distorted $\mathbf{3}_{calc}$ (47 valence electrons) is obtained: on the right-hand side, Figure 5 shows the splitting ($\Delta\epsilon = 0.36$ eV) of the original HOMO into two open-shell orbitals of lower symmetry, one of which is unoccupied (top), and the other one is occupied (bottom) in $\mathbf{3}_{calc}$. Thus, the increased Fe−Fe bond order in **3** results from a smaller number of electrons in $[Fe_3]$ antibonding orbitals.

Mass Spectrometry of $[(Cp^*Fe)_3(\mu_3\text{-}S)_2]$ (3) and $[(Cp^*Fe)_3(\mu_3\text{-}Se)_2]$ (4). More evidence for the correctness of the stated, neutral, composition of **3** and **4** is provided by conventional EI mass spectra (Figures 6 and 7); ionic species such as the anionic 48 clusters should not have been detected by this method. For both compounds, the observed isotopic distribution pattern of the molecular peak $[M]^+$ fits the simulated pattern.

Crystal Structure of $[(Cp^*Fe)_3(SnCl_3)(\mu_3\text{-}Se)_4]\cdot$DME (5). **5** crystallizes in very small yields besides **4**, forming small black platelets. The data of the X-ray diffractometry measurements are given in Table 1. The crystal structure

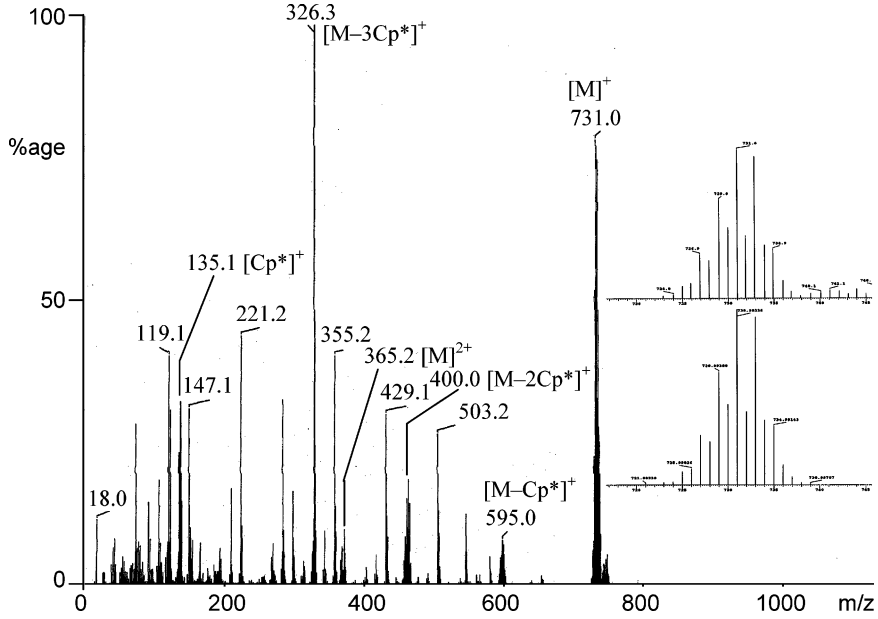

Figure 7. Mass spectrum of **4** (70 eV, 220 °C). The inset shows the isotopic distribution of the observed molecular peak (top) in comparison to the simulated pattern (bottom). Appearance of a larger number of peaks when compared to **3** is due to fragmentation of cocrystallizing **5**.

shows the presence of two independent molecules (**5a** and **5b**), both of which lie on a crystallographic mirror plane and are related by *pseudo* translational symmetry along *c*. The two cluster cores have a similar orientation; the molecules differ primarily in the distortions of their core and by rotation of the Cp* rings. As a consequence of this *pseudo* symmetry, all reflections *hkl* with $l = 2n + 1$ are systematically weak. This is probably reflected in the high value for *R*(int) (Table 1), as half the data have a low I/σ ratio. However this does not prove to be a problem in the refinement of the structure. The data/parameter ratio (all data used in the refinement) was nearly 21:1, and even if one considers only the so-called "observed" reflections, the ratio is still better than 8:1. Although the Fe−C distances are not very precisely determined, a consequence of the presence of several heavy atoms in the structure and also of the expected thermal libration of the Cp* rings, the esds for the Fe···Fe and Fe−Se distances are such that the differences within these distances are statistically very significant, allowing a rather precise comparison of the cores of the two independent clusters. In Figure 8, the molecular structures of **5a** and **5b** are compared (the view direction is the same for both), and respective interatomic distances and angles are given in Table 4. Figure 9 presents a part of the crystal packing illustrating the relative orientation of the two independent molecules on the crystallographic *ac* plane; the latter clearly illustrates the different distortions of the heterocubane units which prevents transformation of **5a** and **5b** into each other by means of symmetry operations.

Both of the crystallographically independent molecules in **5** are based on a $[Fe_3SnSe_4]$ mixed metal heterocubane unit. **5** is an example of the rare type of cubane compound which contains a main group element metal atom besides three transition metal atoms; these are less common than mixed metal heterocubanes including different transition metal

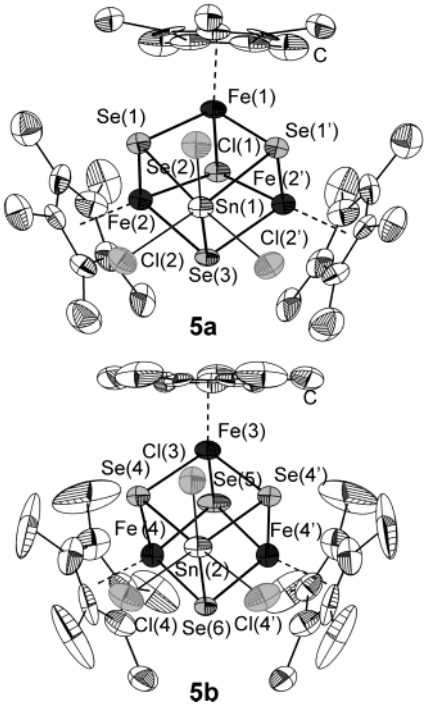

Figure 8. Thermal ellipsoid diagram of the two independent molecules of $[(Cp^*Fe)_3(SnCl_3)(\mu_3\text{-}Se)_4]\cdot$DME (**5**) (**5a**, top; **5b**, bottom); H atoms are omitted for clarity. Ellipsoids are drawn to 50% probability.

elements, such as the recently reported $[(Cp^*Ru)_3(CpTi)(\mu_3\text{-}S)_4]^q$ ($q = 0$, $2+$)[19] or the iron-containing species $[(Cp'Fe)_2\{(CO)_2Mo\}_2(\mu_3\text{-}S)_4]$.[20] The structural parameters in **5a** and **5b** are very similar apart from the Fe···Fe distances and the corresponding Se−Fe−Se or Fe−Se−Fe angles. The lack of significant differences between the two molecules for all other angle and bond ranges and the nearly identical values for the two means of the Fe···Fe distances make the formulation as an ionic pair $[\mathbf{5a}]^+[\mathbf{5b}]^-$ or *vice versa* unlikely. The molecules are, instead, cocrystallizing neutral isomers. The different distortions that affect exclusively very

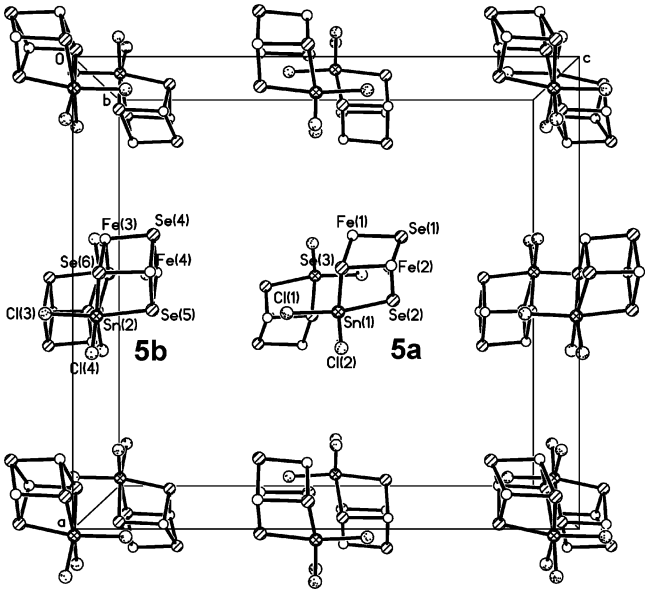

Figure 9. Crystal packing in **5**, viewed along axis *b*; Cp* ligands and the DME molecules are omitted for clarity. Molecules **5a** and **5b** are positioned on the mirror planes at $b = 0.25$ or 0.75 in the crystal lattice and near the 2_1 axes perpendicular to these mirror planes.

Table 4. Selected Distances [Å] and Angles [deg] of **5**

	5a	**5b**
Fe−Se	2.2969(18)−2.3851(19)	2.302(3)−2.368(2)
Fe−C	2.063(11)−2.210(10)	2.072(13)−2.153(12)
Sn−Se	2.6667(17), 2.6726(13)	2.6755(18), 2.6811(13)
Sn−Cl	2.441(3), 2.459(4)	2.433(3), 2.450(4)
Fe(1)···Fe(2)	2.886(2)	
Fe(2)···Fe(2′)	3.476(3)	
Fe(3)···Fe(4)		3.159(2)
Fe(4)···Fe(4′)		2.962(3)
Fe···Fe_{av}	3.083	3.093
Se−Fe−Se	81.23(6)−104.34(7)	90.63(7)−100.94(7)
Fe−Se−Fe	76.36(7)−98.36(9)	78.81(9)−86.18(7)
Fe−Se−Sn	94.60(6)−96.36(6)	94.97(6)−96.57(6)
Se−Sn−Se	77.36(4), 77.63(5)	77.22(4), 77.75(6)
Cl−Sn−Cl	92.14(10), 94.10(15)	91.87(18), 92.68(11)
Cl−Sn−Se_{cis}	93.80(8)−95.31(7)	93.82(8)−95.56(9)
Cl−Sn−Se_{trans}	169.04(11), 169.69(8)	169.25(9), 170.64(12)

soft modes of the molecular cage should thus be considered a consequence of packing effects.

Assuming neutral molecules, both **5a** and **5b** contain 62 valence electrons which allows for 18 electrons at the three Fe centers and 8 electrons at the Sn atom. Consequently, all edges of the [Fe_3Sn] tetrahedra incorporated in the heterocubane cage should be nonbonding. This is in agreement with the Sn···Fe distances (3.718, 3.721 Å in **5a**, 3.711, 3.746 Å in **5b**) and all the large Fe···Fe distances (2.962(3)−3.476(3) Å). Even the two shortest Fe···Fe distances (2.886(2) Å in **5a**) are significantly larger than typical Fe−Fe single bonds as in **3** or **4** (ca. 2.698 Å, s.a.) or in the related 60 electron cluster [$(NO)_{12}Fe_4(\mu_3\text{-}Se)_4$] containing formally six Fe−Fe single bonds (Fe−Fe: 2.705 Å) in the tetrahedral subunit.[21]

It is not trivial to assign formal oxidation states to the metal atoms in **5a** or **5b**, since direct experimental measurements, e.g. by cyclic voltammetry or Mössbauer spectroscopy, have been prevented by the formation of **5** in low yields and as a product mixture in solution (see below). Structural comparison of the distances within the [$SnCl_3$] fragments of four related compounds that also contain mixed metal [$M_3E_4(SnCl_3)$] heterocubane cages (M = W, Mo; E = S, Se), [$M^{IV}{}_3(NCS)_9(\mu_3\text{-}E)_4(Sn^{II}Cl_3)$]$^{6-}$ [22−25] gives evidence for the presence of Sn^{II} in the $SnCl_3$ fragments of **5**: In the quoted systems, the influence of the nature of the transition metal as well as the chalcogenide ligand on the Sn−E bond length leads to a shortening of ca. 0.1 Å on going from M = W to Mo, for both E = S and Se (M = W, Sn−S_{av}, 2.741 Å, Sn−Se_{av}, 2.847 Å; M = Mo, Sn−S_{av} 2.649 Å, Sn−Se_{av}, 2.774 Å). Extrapolation to a related first row transition metal selenide cluster would give a value close to the observed average Sn−Se distance of 2.673 Å in **5**. Assignment of the tin as Sn^{II} requires all three iron centers to be Fe^{IV}, the same oxidation state as for the abovementioned Mo/Sn/E and W/Sn/E clusters, but perhaps rather unexpected for an iron selenide compound. However, there are some iron sulfide and one iron selenide heterocubane type clusters that formally contain Fe^{IV} centers, [$(CpFe)_4(\mu_3\text{-}S)_4$]$^{q+}$ ($q = 1, 2$),[26] [{$(S_2C_2(CF_3)_2)Fe$}$_4(\mu_3\text{-}S)_4$]$^{q-}$ ($q = 0, 1, 2$),[27] and [$(CpFe)_4(\mu_3\text{-}Se)_4$]$^{3+}$,[28] in which the occurrence of such extreme formal oxidation states was explained by removal of electrons from MOs with a significant contribution from Cp orbitals. Accordingly, the Cp* ligand, which is known to have an even higher oxidation potential,[29] could allow for a similar situation in the iron/tin selenide cluster **5**.

Good evidence for the correctness of the formulated electron number, leading to the high formal oxidation states at the Fe atoms, is provided by comparison of the Fe−Se distances observed in **5** with those of related Fe−Se cluster compounds. In [$(CpFe)_4(\mu_3\text{-}Se)_4$]$^{3+}$,[28] formally containing $Fe^{III}/Fe^{IV}/Fe^{IV}/Fe^{IV}$, the Fe−Se bonds range between 2.260(3) and 2.350(3) Å (2.309 Å on average), in agreement with the values obtained in **5** (2.2969(18)−2.3851(19) Å, 2.338 on average). Slight elongation of the bonds in **5** when compared to the cited compound is expected due to larger terminal ligands (Cp* vs Cp). Available data on further related compounds concern clusters with lower oxidation states at the Fe centers, which is again reflected by the according Fe−Se distances. Examples are [$(ClFe)_4(\mu_3\text{-}Se)_4$]$^{2-}$ ($Fe^{II}/Fe^{II}/Fe^{III}/Fe^{III}$; Fe−Se: 2.411 Å on average),[30] [{$(EtS)Fe$}$_4(\mu_3\text{-}Se)_4$]$^{3-}$ ($Fe^{II}/Fe^{II}/Fe^{II}/Fe^{III}$; Fe−Se: 2.441 Å on average),[31] or [{$(CO)_3Fe$}$_4(\mu_3\text{-}Se)_4$] (Fe^{II}; Fe−Se: 2.446 Å on average).[32]

Electrospray/Ionization (ESI) Mass Spectrometry of [$(Cp^*Fe)_3(SnCl_3)(\mu_3\text{-}Se)_4$]·DME (5). By electrospray/ionization (ESI) mass spectrometry it was shown that **5** is, however, the dominant species within the reaction solution

(27) (a) Balch, A. L. *J. Am. Chem. Soc.* **1969**, *91*, 6962−6967. (b) Lemmen, T. H.; Kocal, J. A.; Lo, F. Y.-K.; Chen, M. W.; Dahl, L. F. *J. Am. Chem. Soc.* **1981**, *103*, 1932−1941.
(28) Ogino, H.; Tobita, H.; Yanagisawa, K.; Shimoi, M.; Kabuto, C. *J. Am. Chem. Soc.* **1987**, *109*, 5847−5848.
(29) Kölle, U.; Khouzami, F. *Angew. Chem., Int. Ed. Engl.* **1980**, *19*, 640−641.
(30) Ahle, A.; Dehnicke, K.; Maichle, C.; Strähle, J. *Z. Naturforsch.* **1994**, *94b*, 434−436.
(31) Ciurli, S.; Yu, S.-b.; Holm, R. H.; Srivastava, K. K. P.; Münck, E. *J. Am. Chem. Soc.* **1990**, *112*, 8169−8171.
(32) Nelson, L. L.; Lo, F. Y.-K.; Rae, A. D.; Dahl, L. F. *J. Organomet. Chem.* **1982**, *225*, 309−329.

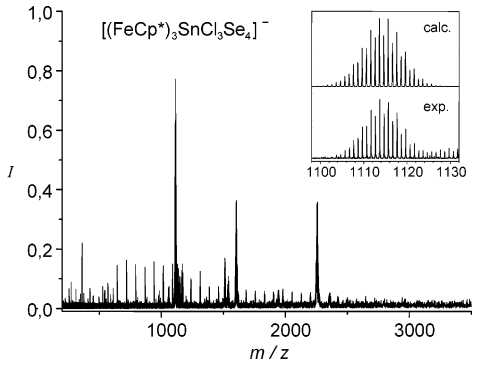

Figure 10. Negative-ion electrospray mass spectrum of a DME solution containing **5**. In the inset the measured parent ion peak is contrasted to the simulated isotope distribution.

yielding **4** and **5** according to Scheme 1 (E = Se), at room temperature; this is in contrast to the observed crystal yields and might give evidence for an equilibrium between **4** and **5** in solution which is shifted toward **4** due to significantly lower solubility of this species at lower temperatures. Figure 10 shows the ESI spectrum taken in the negative-ion mode.

Clearly, the molecular anion of **5** is the most prominent peak in the spectrum indicating that the cluster is present as such in solution. Regarding the charge state it cannot be ruled out that the cluster was reduced electrochemically upon spraying the solution. Such electrochemical oxidation/reduction processes in an electrospray setup have been investigated by the groups of Kebarle[33] and Van Berkel.[34] Specifically, it has been observed that Fe(III) compounds are reduced to Fe(II)[35] in the negative-ion mode of an electrospray source. In that sense the FeSeSn heterocubane compound **5** may appear very prone to such a reduction step to form an anionic species from a neutral molecule. This is in accordance with the absence of cations such as Li^+ which would be easily detected by X-ray crystallography due to their tendency to be coordinated by DME molecules. The less intense peaks do not accord to aggregates that can be viewed as simple fragments or oligomers of **5**, nor do they accord to any of the peaks occurring in the EI mass spectrum of **4** (see Figure 7); however is possible to assign hypothetic compositions to the peaks, e.g. $[(Cp^*Fe)_4Sn_4Se_{12}Cl_2]$ to the heaviest one at $m/z = 2257$.

5 is the first example of the formation of a ternary M/Sn/E compound by reaction of chalcogenostannate anions with organometallic complexes in aprotic solvents. It is not clear yet whether the Sn−Se bonds have remained from the reactant $[Sn_2Se_6]^{4-}$ or whether a preformed "$[(Cp^*Fe)_3(\mu_3\text{-}Se)_4]^{+}$" species could have trapped an $[SnCl_3]^-$ ion resulting from the $[Sn_2Se_6]$ fragmentation in the reaction mixture. The latter is perhaps more likely since the quoted W/Sn/Se or Mo/Sn/Se clusters were synthesized from incomplete heterocubane type complexes $[M_3Se_4(H_2O)_9]^{4+}$.[22−25]

(33) Blades, T.; Ikonomou, M. G.; Kebarle, P. *Anal. Chem.* **1991**, *63*, 2109−2114.
(34) Van Berkel, G. J.; Zhou, F. *Anal. Chem.* **1995**, *67*, 2916−2923.
(35) Mollah, S.; Pris, A. D.; Johnson, S. K.; Gwizdale, A. B., III; Houk, R. S. *Anal. Chem.* **2000**, *72*, 985−991.

Summary

1-Aminoethylammonium salts of $[Sn_2E_6]^{4-}$ anions, $[enH]_4[Sn_2S_6]$ (**1**) and $[enH]_4[Sn_2Se_6]\cdot en$ (**2**), with $FeCl_2$/LiCp* have been shown to be suitable reactants for the formation of Cp* ligated, partially oxidized Fe/S or Fe/Se complexes: $[(Cp^*Fe)_3(\mu_3\text{-}S)_2]$ (**3**) and $[(Cp^*Fe)_3(\mu_3\text{-}Se)_2]$ (**4**). The distortedly trigonal bipyramidal clusters feature a rare, odd electron number of 47 valence electrons which has been confirmed by mass spectrometry, cyclic voltammetry, magnetic measurements, and DFT calculations. The use of **2** additionally allowed for the isolation of the first ternary Fe/Sn/Se complex from the reaction of a chalcogenostannate salt toward an organometallic complex. Compound $[(Cp^*Fe)_3(SnCl_3)(\mu_3\text{-}Se)_4]\cdot$DME (**5**) is structurally related to some M/Sn/E complexes (M = Mo, W; E = S, Se), but represents the first example of this type containing 3d metal atoms or Cp* ligands. The structural parameters give evidence for the presence of Sn^{II} in the mixed metal heterocubane unit, and thus for a formal oxidation state of +IV for the Fe centers. However, it seems to be more reasonable to discuss an overall oxidation of the system, i.e. removal of electrons from MOs with significant contribution from Cp* orbitals as described for highly oxidized, Cp ligated Fe_4E_4 clusters.

Experimental Section

Experimental Methods. All reaction steps were carried out with strong exclusion of air and moisture either in a dry nitrogen atmosphere or under argon (glovebox). All solvents were dried and freshly distilled prior to use. $[enH]_4[Sn_2S_6]$ and $[enH]_4[Sn_2Se_6]\cdot en$ were prepared as previously described.[12] For the syntheses of **3**−**5**, $FeCl_2$ (0.050 g, 0.4 mmol; **3**) and LiCp* (0.056 g, 0.4 mmol) were stirred in 3 mL of DME for 20 min at room temperature, resulting in the formation of a brownish suspension.

Preparation of $[(Cp^*Fe)_3(\mu_3\text{-}S)_2]$ (3). $[enH]_4[Sn_2S_6]$ (0.072 g, 0.11 mmol) was added to the suspension at room temperature. After stirring for 12 h, an insoluble black precipitate was removed to leave a dark brown solution. After storing of the filtrate at −40 °C for 24 h, black rhombic crystals of **3** were obtained. Yield: 0.022 g (0.03 mmol; 26% based on Fe). MS (70 eV) of $[M]^+$ [*m*/*z*], (%): 637 (100). C,H analysis [%]: obsd, C 56.15, H 7.16; calcd for $C_{30}H_{45}Fe_3S_2$, C 56.54, H 7.12.

Preparation of $[(Cp^*Fe)_3(\mu_3\text{-}Se)_2]$ (4) and $[(Cp^*Fe)_3(SnCl_3)(\mu_3\text{-}Se)_4]\cdot$DME (5). $[enH]_4[Sn_2Se_6]\cdot en$ (0.100 g, 0.11 mmol) was added to the suspension at room temperature, and the mixture was stirred for 14 h. After removal of an insoluble black precipitate, the dark brown filtrate was stored at −40 °C. Dark purple crystals of **4** formed at the glass wall of the Schlenk tube within 2 weeks together with small amounts of very small black blocks of **5** that were reproducibly embedded in a drop of a colorless, oily liquid. Yields: **4**, 0.016 g (0.02 mmol; 16% based on Fe); **5**, 0.002 g (1.66 μmol; 1% based on Fe). MS (70 eV) of $[M]^+$ [*m*/*z*], (%): **4**, 731 (78). C,H analysis [%]: **4**, obsd, C 48.99, H 6.24; calcd for $C_{30}H_{45}Fe_3Se_2$, C 49.28, H 6.29.

X-ray Diffractometry. The data were obtained on a Bruker SMART APEX CCD diffractometer with graphite monochromated Mo Kα radiation ($\lambda = 0.71073$ Å) at 200 K. Empirical absorption corrections were performed using the SADABS program.[36] The

(36) Sheldrick, G. M. *SADABS (the Siemens Area Detector Absorption Correction)*; University of Göttingen: Göttingen, Germany, 1996.

structures were solved by direct methods (SHELXS-86)[37] and were refined employing full-matrix least-squares on F^2 (SHELXL-97).[37]

Methods of the Theoretical Investigations. The density functional theoretical (DFT)[13] investigations were undertaken by means of the program system TURBOMOLE[38] using the RIDFT program[39] with the Becke−Perdew (B−P) functional[40] and the gridsize m3. This method was formerly proved to be the most suitable for electron rich transition metal compounds. Basis sets were of TZVP quality (TZVP = triple-ζ valence plus polarization).[38] For modeling the Fe_3E_2 compounds, the highest possible idealized symmetry without sterically hindered CH_3 groups of the Cp* ligands would be C_3. However, in order to allow the system to undergo the experimentally observed distortion for the 47 electron species, the simultaneous optimizations of geometric and electronic structures were performed without symmetry restrictions, i.e. in C_1 symmetry. The existence of local minima on the energy hyperface was checked by slight distortion of the converged C_1 symmetric structures along soft modes followed by new optimization runs. All structures reconverged into the presented species. Orbital plots were drawn by means of the program gOpenmole.

Spectroscopy. Mass spectra were recorded on a mass spectrometer MS 8230 (Finnigan) at 70 eV. Electron paramagnetic resonance spectra were recorded with a Bruker ESP300E X-band spectrometer (9.5 GHz) equipped with a rectangular cavity and an Oxford ESR900 cryostat.

Electrochemical Methods. Electrochemical experiments were done on a CH Instruments 660 electrochemical workstation. The cyclic voltammogram of **3** was measured at a scan rate of 0.100 $V \cdot s^{-1}$ on a solution of **3** in CH_2Cl_2 (c = 1.5 $mmol \cdot L^{-1}$), using ($^nBu_4N$)(PF_6) (c = 0.2 $mm \cdot L^{-1}$) as supporting electrolyte, and referenced to $Fc^{0/+}$. A platinum wire counter electrode, a glassy carbon working electrode, and a Ag/AgCl reference electrode were used. All manipulations were carried out under argon or nitrogen.

Static Magnetic Susceptibility. The static magnetic susceptibility was measured with a SQUID magnetometer (Magnetic Properties Measurement System) by Quantum Design for a field strength of 10 kOe and 1 kOe in the temperature range between 2 and 300 K. The sample mass was (5.2 ± 0.1) mg in a sealed quartz tube.

Electrospray/Ionization Mass Spectrometry. Electrospray mass spectra were taken on a Fourier transform ion cyclotron resonance (FT-ICR) mass spectrometer (Bruker Daltonics).

Acknowledgment. This work has been supported by the State of Baden-Württemberg (Margarete-von-Wrangell habilitation fellowship for S.D.), by the Deutsche Forschungsgemeinschaft, and by the Fonds der Chemischen Industrie. Generous support from Prof. Dr. D. Fenske, Prof. Dr. R. Ahlrichs, Prof. Dr. A. Powell, and Prof. Dr. E. Dormann is gratefully acknowledged. We are very indebted to D. Müller for recording the mass spectra and Prof. Dr. T. Meade for the use of the electrochemical workstation.

Supporting Information Available: Crystallographic data in CIF format. This material is available free of charge via the Internet at http://pubs.acs.org.

IC034876T

(37) Sheldrick, G. M. *SHELXTL 5.1*; Bruker AXS Inc.: Madison, WI 1997.
(38) (a) Ahlrichs, R.; Bär, M.; Häser, M.; Horn, H.; Kölmel, C. *Chem. Phys. Lett.* **1989**, *162*, 165−169. (b) Treutler, O.; Ahlrichs, R. *J. Chem. Phys.* **1995**, *102*, 346−354.
(39) (a) Eichkorn, K.; Treutler, O.; Öhm, H.; Häser, M.; Ahlrichs, R. *Chem. Phys. Lett.* **1995**, *242*, 652−660. (b) Eichkorn, K.; Weigend, F.; Treutler, O.; Ahlrichs, R. *Theor. Chim. Acta* **1997**, *97*, 119−124.
(40) (a) Becke, A. D. *Phys. Rev. A* **1988**, *38*, 3098−3109. (b) Vosko, S. H.; Wilk, L.; Nusair, M. *Can. J. Phys.* **1980**, *58*, 1200−1205. (c) Perdew, J. P. *Phys. Rev. B* **1986**, *33*, 8822−8837.